RESEARCH ARTICLE

Effect of Graphene Nanoribbons (TexasPEG) on locomotor function recovery in a rat model of lumbar spinal cord transection

C-Yoon Kim[1, 2, *, #], William K. A. Sikkema[3, #], Jin Kim[2], Jeong Ah Kim[4], James Walter[5], Raymond Dieter[5], Hyung-Min Chung[1], Andrea Mana[6], James M. Tour[3], Sergio Canavero[6, *]

1 Department of Stem Cell Biology, School of Medicine, Konkuk University, Seoul, Korea
2 Department of Laboratory Animal Medicine, College of Veterinary Medicine, Seoul National University, Seoul, Korea
3 Department of Chemistry, Department of Materials Science and NanoEngineering, and The NanoCarbon Center, Rice University, Houston, TX, USA
4 Biomedical Omics Group, Korea Basic Science Institute, Cheongju-si, Chungbuk, Korea
5 Research Service, Hines Veterans Administration Hospital, Hines, IL, USA
6 HEAVEN/GEMINI International Collaborative Group, Turin, Italy

Funding: *This research was supported by a grant from the National Research Foundation (NRF) funded by the Korean government (NRF-2015M3A9C7030091 and NRF-2015R1C1A1A02037047).*

Abstract

A sharply transected spinal cord has been shown to be fused under the accelerating influence of membrane fusogens such as polyethylene glycol (PEG) (GEMINI protocol). Previous work provided evidence that this is in fact possible. Other fusogens might improve current results. In this study, we aimed to assess the effects of PEGylated graphene nanoribons (PEG-GNR, and called "TexasPEG" when prepared as 1wt% dispersion in PEG600) *versus* placebo (saline) on locomotor function recovery and cellular level in a rat model of spinal cord transection at lumbar segment 1 (L_1) level. *In vivo* and *in vitro* experiments (n = 10 per experiment) were designed. In the *in vivo* experiment, all rats were submitted to full spinal cord transection at L_1 level. Five weeks later, behavioral assessment was performed using the Basso Beattie Bresnahan (BBB) locomotor rating scale. Immunohistochemical staining with neuron marker neurofilament 200 (NF200) antibody and astrocytic scar marker glial fibrillary acidic protein (GFAP) was also performed in the injured spinal cord. In the *in vitro* experiment, the effects of TexasPEG application for 72 hours on the neurite outgrowth of SH-SY5Y cells were observed under the inverted microscope. Results of both *in vivo* and *in vitro* experiments suggest that TexasPEG reduces the formation of glial scars, promotes the regeneration of neurites, and thereby contributes to the recovery of locomotor function of a rat model of spinal cord transfection.

Key Words: *nerve regeneration; spinal cord transfection; spinal cord fusion; GEMINI; TexasPEG; graphene nanoribbons*

Correspondence to:
C-Yoon Kim, V.M.D. or Sergio Canavero, M.D., vivavets@gmail.com or sercan@inwind.it.

#These authors equally contributed to this work.

orcid:
0000-0003-1199-8024 (C-Yoon Kim)

doi: *10.4103/1673-5374.235301*

Accepted: *2018-05-31*

Introduction

Despite more than a century of intensive research, spinal cord injury (SCI) remains an incurable condition and often causes devastating sequelae. Although a host of experimental therapies have been deployed over the years, none has made it to the clinic, including stem cells (Silva et al., 2014; Kim et al., 2017b). The rationale for almost all attempts at reversing spinal injury has been to counteract the detrimental effects of necrosis, along with cysts and scars, by either allaying local inhibition or fostering regrowth of long axons in the damaged white matter. All these studies led to only limited available treatment. Progress has been made in the neurorehabilitation setting, with the introduction of exoskeletons for low-level spinal cord lesions and the resulting ambulation assist (Miller et al., 2016). Brain-computer interfaces are showing early promise, especially for high-level spinal lesions (Lebedev and Nicolelis, 2017) and electrical spinal cord stimulation can activate motor programs in paraplegic patients (Minassian and Hofstoetter, 2016). However, none of these technologies can currently restore full, behaviorally effective sensorimotor function. The need for a biological cure remains imperative.

In 1963, US neurosurgeon Dr. Freeman proved that a sharply severed thoracic spinal cord can achieve motor recovery in rodents and dogs if enough time is permitted (months) and fiber regrowth was observed histologically (Freeman, 1963; Canavero et al., 2016). In light of these results, Dr. Freeman speculated that a dorsal injury leading to paraplegia could be cured if the injured segment was removed, along with a vertebrectomy (spinal shortening) or even multiple diskectomies, and the two freshly severed cord stumps approximated. In fact, when he carried out this procedure in animals, locomotor function was partially restored. For unclear reasons, this data went ignored by the spinal cord community at large (Canavero and Ren, 2016). Certainly, the interval of time necessary for this recovery, translated to the human subject, amounts to a few years. This was confirmed when two surgical groups removed the injured segment in two paraplegics and filled the gap with collagen or peripheral nerve bridges: partial motor function recovery was seen > 1 year later (up to 4 years) (Goldsmith et al., 2005; Tabakow et al., 2014). This suggests that, if a method should be found whereby the fresh stumps of a cord submitted to cordectomy could be made to communicate electrophysiologically (*i.e.*, spinal cord fusion), a cure for SCI could result. In fact, the vertebral column can be surgically shortened (by corporectomy or multiple diskectomies), and the two freshly severed cord stumps approximated. Still, the process must be accelerated to make it clinically practical.

In 2013, the GEMINI spinal cord fusion protocol was first described (Canavero, 2013). The aim is to fuse a sharply transected spinal cord and reverse the resulting motor deficit. The protocol recognizes that sensorimotor function in mammals is subserved by a cellular "highway" embedded in the gray matter of the spinal cord and that protecting the neurons that make up this pathway at the point of operative transection would foster sprouting of new neural connections between the stumps of the transected spinal cord (Canavero et al., 2016). Special substances, classified as membrane fusogens (*e.g.*, poly(ethylene glycol), PEG), can acutely restore the integrity of sharply severed nerve fibers or seal the membrane of damaged neurons, reducing cell death in the spinal cord (Canavero et al., 2016; Ye et al., 2016). This effect requires topical application to be maximally effective. In 2016, proof-of-principle animal studies confirmed the feasibility of fusing a sharply transected, cervical (C_5) or dorsal (T_{10}) spinal cord with objective restoration of electrical transmission and recovery of ambulation, first in mice (Kim, 2016; Ye et al., 2016; Kim et al., 2017a), then in rats (Kim et al., 2016c), and finally in a single dog (Kim et al., 2016b). An adequately powered, randomized, controlled study in rats later confirmed these initial findings (Ren et al., 2017). Motor function recovered in all these studies. On the other hand, parenteral administration of PEG has not proven particularly effective at reversing experimental contusive SCI, although in those studies PEG was administered within 24 hours of SCI (Laverty et al., 2004; Olby et al., 2016). While a human trial is certainly warranted, intravenous administration of PEG would be useless in the chronic setting.

We theorized that PEGylated graphene nanoribbons (PEG-GNR) could reestablish anatomophysiological continuity of the transected spinal cord. TexasPEG is a mixture where the nanoribbons are diluted as a 1wt% dispersion in 600 Da PEG. TexasPEG has been shown to have favorable neuronal effects in SCI studies, as per the GEMINI protocol (Kim et al., 2016a). These nanoribbons are chemically modified with PEG chains emanating from their edges, yet the basal planes are pristine so they are highly electrically conductive. We have shown these planes to stimulate neuronal growth on their surfaces and to be nontoxic (Sahni et al., 2013). TexasPEG may produce a microenvironment that is conducive to neuronal growth, providing a scaffold that can electro-positionally inform the growth cones of neuronal processes, and facilitate reconnection of closely appositioned severed nerve fibers.

In order to test the fusogen administered directly to the cord in the clinic, animal evidence is required by regulatory bodies. Preliminary animal histologic analysis with PEG revealed that the two approximated stumps of the transected spinal cord regrew nerve fibers across the interface, but the extent of regrowth was not quantified (Kim et al., 2017a). Moreover, the exact cellular mechanism of the recovery remains unexplored.

Here, we aim to provide evidence that TexasPEG can restore motor function after complete L_1 spinal cord transections and immediate treatment. We also aim to elucidate the biological mechanism of recovery using immunohistochemistry and in vitro studies. In our prior work, we tested both C_5 and T_9 complete sharp lesions of the spinal cord (Kim et al., 2016a; Ye et al., 2016). These high-level spinal cord lesion sites are characterized by both caudal and rostral perfusion. In the current study, we created an L_1 lesion site which has the limitation of only rostral perfusion, a possible ischemia-inducing hindrance to neuronal survival in the gray matter, which is critical for spinal fusion.

Materials and Methods

The PEG-GNRs (TexasPEG)

In this study, PEGylated graphene nanoribbons (TexasPEG) was used (see details on preparation and characterization in a previous study (Sikkema et al., 2017)). A brief description of the protocol and characterization are described in **Figure 1**.

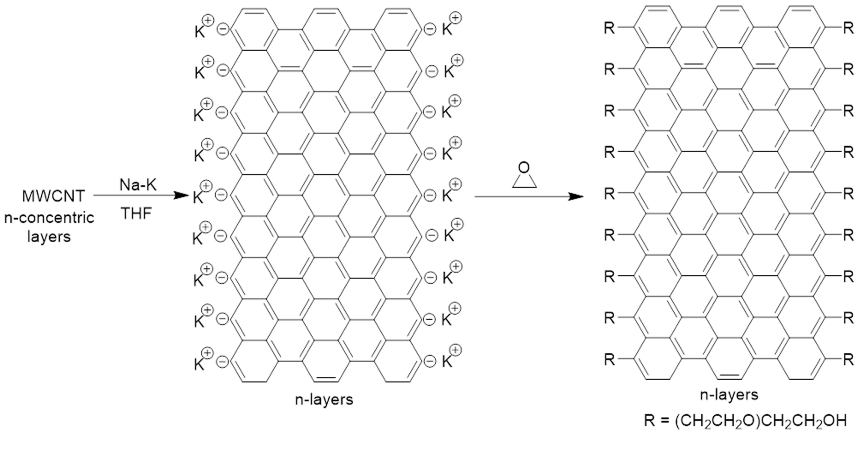

Figure 1 Multiwalled carbon nanotubes (MWCNTs) consist of concentric layers of carbon nanotubes.
Treatment with sodium-potassium alloy in tetrahydrofuran (THF) solvent afforded the longitudinally split nanotubes that become graphene nanoribbons (GNR), and they bear anions at the edge. The counterions are shown as potassium but they could also be sodium. This solution is then treated with ethylene oxide to promote PEGylation from the edges of the GNRs, leaving the basal planes intact, and therefore highly conductive. These constructs are approximately 6–8 GNR layers per stack which is 2–4 nm thick, and the figures are not shown to scale; the GNRs are ~200–250 nm wide and 3–5 m long. The length of the polyethylene glycol (PEG) chains is very difficult to determine due to the inhomogeneity of lengths.

***In vivo* assessment**

Spinal cord transection and treatment

The experiment was carried out in accordance with animal ethics committee guidelines and was approved by the Institutional Animal Care and Use Committee of the Konkuk University (approval No. KU15135). Female Sprague-Dawley rats (Young bio, Seoul, Korea), weighing 250–280 g, were anesthetized using zoletil and xylazine (3:1 ratio, 1 mL/kg). Spinal laminectomy was performed at L_1 site. Briefly, the muscles overlying the vertebral column were cut open to expose the vertebral column T_{13}–L_2; the L_1 spine segment was carefully removed. After gently raising the spinal cord with a spinal cord hook (Fine Science Tools, Vancouver, Canada), severance was performed with surgical sharp blades #11; the gap was confirmed by passing the hook throughout. The animals were randomly divided into two groups (control and TexasPEG, n =10 for each group) and treated with either 50 μL of PBS or TexasPEG respectively, directly applied on the severance site of the spinal cord. Then, the muscle and fascia were sutured and the skin was closed. Dextrose (2.5%) and 0.45% sodium chloride (20 mL/kg; Haflsol, Daehan, Seoul, Korea) was administered daily *via* a tail vein catheter. To confirm the disappearance of the motor improvement following spinal re-transection, all groups of animals were re-anesthetized and the L_1 site was incised after 5 weeks of behavioral analysis. The spinal cord at L_1 level was transected in the same manner as described above, and then sutured without any treatment.

Behavioral assessment

The Basso Beattie Bresnahan (BBB) locomotor rating scale (Basso et al., 1995) was used to assess locomotor function recovery in an open field; *i.e.*, with rats left to themselves to move and feed in a spacious pen. Two independent, blinded observers evaluated the spinal cord sensory and motor function of the animals after spinal cord transection. Before testing, the animals' bladders were expressed because spontaneous bladder contraction often accompanies hind limb activity. The rats were placed in an open field and were observed for 5 minutes. Functional recovery was analyzed by measuring the BBB score twice a week. Functional recovery was analyzed twice a week for up to 5 weeks (+1 day).

Immunohistochemistry

All rats were sacrificed at 5 weeks (+1 day) after operation. The spinal cord was isolated and fixed with 4% paraformaldehyde. During autopsy, the spinal cord above and below the level of injury was observed and the diameter was measured to determine if atrophy was present. Tissue samples were rinsed with PBS and stored in PBS with 30% sucrose overnight. Tissue samples were embedded in O.C.T. compound (Sakura Finetek, Tokyo, Japan) media; 10 μm longitudinal sections were obtained. The sections were incubated with primary antibodies anti-neurofilament 200 (1:100; Sigma, St. Louis, MO, USA) and anti-glial fibrillary acidic protein (1:1000; Chemicon, Tenecula, CA, USA) for 72 hours at 4°C. The sections were then washed with PBS and incubated with Alexa 488 or 594 conjugated secondary antibody (Goat IgG, 1:1000; Molecular Probes, Eugene, OR, USA) for 1 hour at room temperature and mounted with 4′,6-diamidino-2-phenyindole (DAPI). Each evaluation proceeded at the interface and periphery of the injured spinal cord. In the periphery of the injured area, immunohistochemical staining with anti-glial fibrillary acidic protein (GFAP; an astrocytic scar-related marker) was performed in the gray matter, and immunohistochemical staining with anti-neurofilament 200 (NF200; neuron marker) in the white matter. For each sample, three images of the injured area were randomly selected. Images were acquired using a fluorescence microscope fitted with a digital camera system (Nikon, Tokyo, Japan) for quantitative analyses using Adobe Photoshop CS5 (Adobe Systems, San Jose, CA, USA) software. Attention was given to ensure identical settings for fluorescence exposure, amplifier gain and cut off across all images.

***In vitro* assessment**

Cell culture

SH-SY5Y cells (KCLB, Seoul, Korea) were cultured and maintained in Dubelcco's Modified Eagle Media (DMEM) Ham's F-12 (DMEM/F12) (Sigma-Aldrich, St. Louis, MO, USA) supplemented with 15% heat inactivated fetal bovine serum (Sigma-Aldrich) and 1% penicillin/streptomycin (Sigma-Aldrich). The cells were incubated at 37°C in a humidified incubator containing 5% CO_2. For differentiation of SH-SY5Y cells, cells were treated with 10 μM all-trans retinoic acid (RA) (Sigma-Aldrich) with 5% fetal bovine serum in DMEM/F12 media. The retinoic acid was dissolved (10 mM) in dimethyl sulfoxide, and freshly diluted further in culture medium.

Fabrication of the microfluidic device

A microfluidic device was fabricated with a poly(dimethylsiloxane) (PDMS) replica molding using a standard soft lithography from a patterned SU-8 silicon wafer (**Figure 2**). Briefly, SU-8 photoresist (Microchem Corp., Newton, MA, USA) was spin-coated at a thickness of about 200 μm on a Si wafer. After baking and rinsing, PDMS prepolymer mixed with a curing agent at a weight ratio of 10: 1 (Sylgard® 184, Dow Corning Co., Midland, MI, USA) was poured onto the master and cured for 2 hours at 80°C. PDMS replica was peeled off from the master and an inlet and an outlet hole were punched out of the PDMS replica. After sterilization by autoclave, the PDMS layer was bonded onto a coverslip by an air plasma treatment (150 W, 50 seconds) to form a closed channel (Femto Science Inc., Covance, Korea). The single device has three rectangular microchannels, one for gel and two for media. The channel dimension for gel is 1.2 mm wide, 16 mm long and the media channel is 1 mm wide, 33 mm long, respectively. A single pair of reservoirs (6 mm in diameter) is shared at the end of the two media channels. Each hydrogel channel is defined by a row of trapezoid-shaped posts that separate neighbouring channels.

3D culture and microscopic evaluation

To evaluate the effect of TexasPEG on neurite growth at the *in vitro* level, we developed a 3D culture using matrigel and microchips. Single SH-SY5Y cells were suspended in Matrigel™/serum free DMEM (BD, Franklin Lakes, NJ, USA) (1:1) at a concentration of 1×10^6 cells/mL. For graphene treatment, TexasPEG was diluted in the mixture to a final concentration of 0.2%. The solution was then injected gently into an individual chamber of a microchip and allowed to solidify for 1 hour at 37°C in a humidified incubator containing 5% CO_2. Fifty microliter of differentiation media was added gently to each chamber and the media was changed twice a day. To assess neurite growth from SH-SY5Y cells after 72 hours of incubation, phase contrast images at 200× magnification were captured using a Zeiss inverted microscope and Axiovision software (Carl Zeiss, Jena, Germany) for each group, and the mean neurite length of each single cell was calculated using ImageJ software (NIH, Bethesda, MD, USA) on at least 50 randomly selected cells. For the analysis, a neurite was defined as a cell process greater than 20 μm, for branching neurites, only the longest branch was traced and only cells with the entire cell body and neurite in the field of view were included.

Statistics

Statistical analyses were conducted using the Statistical Analysis System software (SAS, version Enterprise 4.0; SAS Korea, Inc., Seoul, Korea), Data are presented as the mean ± SEM. All statistics were calculated using independent samples *t*-test or one-way analysis of variance (ANOVA) with the least significant differences (LSD) test for *post hoc* analysis. A value of $P < 0.05$ was considered statistically significant.

Results

Behavioral change of rats

BBB scores across 5 weeks were compared between TexasPEG and control groups (**Figure 3**). BBB scores at 3–5 weeks in the TexasPEG group were significantly higher than those in the control group ($P < 0.05$ or $P < 0.01$). Locomotor function recovery in the control group plateaued after 1 week, while the TexasPEG group showed continuous restoration of motor function for 5 weeks. To confirm whether the restored motor function was actually due to spinal cord regeneration, the spinal cord (L_1) was re-transected at the end of these 5 weeks. Paralysis was induced again in both groups (**Figure 3**). Interestingly, extensive atrophy of the lower part of the L_1 lesion was observed (**Additional Figure 1**). The spinal cord below the level of injury (caudal) showed an atrophic morphology. In contrast, the spinal cord above the level of injury (rostral) demonstrated no atrophy.

Scar formation and axonal regrowth

Scar formation and axonal regrowth were histologically assessed. GFAP immunoreactivity was detected at the boundary area and at the periphery (**Figure 4A**; hematoxylin-eosin staining is shown in **Additional Figure 2**). The severity of glial scar formation was analyzed semi-quantitatively (**Figure 4B**). Control animals exhibited a significantly increased amount of and complex patterns of glial scars with prominent bundles of thick astrocytic processes (**Figure 4A**). Instead, GFAP immunoreactivity was markedly attenuated in the TexasPEG group ($P < 0.001$). Moreover, the thickness and shape of astrocytic processes at the periphery were obviously different from those at the boundary area.

To measure axonal regrowth at the lesion site, NF200 immunofluorescence was evaluated in the boundary area of the white matter (hematoxylin-eosin staining is shown in **Additional Figure 2**). Only a small number of axon profiles were observed in the control group, whereas a strong immunoreactivity was detected in the TexasPEG group ($P < 0.001$) (**Figure 4C** and **D**). Moreover, the axon profiles of the control group showed an incomplete form with an intermediate break (**Figure4C**). In the TexasPEG group, some of axons were dystrophic with swelling, but the majority showed continuous and linear extended shapes, including multiple branches (**Figure 4C**).

In vitro assessment results

Neurite growth of SH-SY5Y cells was assessed *in vitro*. 3D culture was carried out using matrigel and microchip to investigate the influence of three-dimensional TexasPEG by excluding an interference effect caused by surface adhesion in 2D culture (**Figure 5A**). Neurites were observed in all cells of each group, and no significant effect was observed on the ratio of neurites expressing cells. Interestingly, TexasPEG-treated cells were longer in morphology than control cells ($P < 0.001$) and they had multiple prominent neurites (**Figure 5B**). This is consistent with the axonal regrowth profile of the *in vivo* results.

Discussion

We confirmed previous studies in our group (see introduction) that a severed spinal cord can be "fused" with behavioral recovery. The TexasPEG group showed a significant recovery as compared to the control group after 2 weeks with the maximal recovery at 5 weeks: recovery is attributable to spinal reconstruction at the lesion level. This was confirmed by re-transection at L_1 level and attendant loss of locomotor function.

The key to spinal cord fusion is a sharp severance of the cords themselves, with its attendant minimal damage to the cord gray and white matter: a typical force generated by creating a sharp transection is less than 10 N versus approximately 26,000 N experienced during SCI, a 2600× difference (Canavero, 2015).

The control group with only the L_1 lesion reached a BBB score of 3.90 ± 0.53, demonstrating some recovery from a sharp cut at a relatively short follow-up (5 weeks). The behavioral recovery in the present and previous studies can be explained by considering how the spinal cord processes motor programs. About 20 million fibers pass through the spinal cord, with approximately 1 million of descending pyramidal fibers (Canavero, 2015; Canavero et al., 2016). It is generally believed that the long-range corticospinal (pyramidal) fibers are mainly responsible for activating the spinal

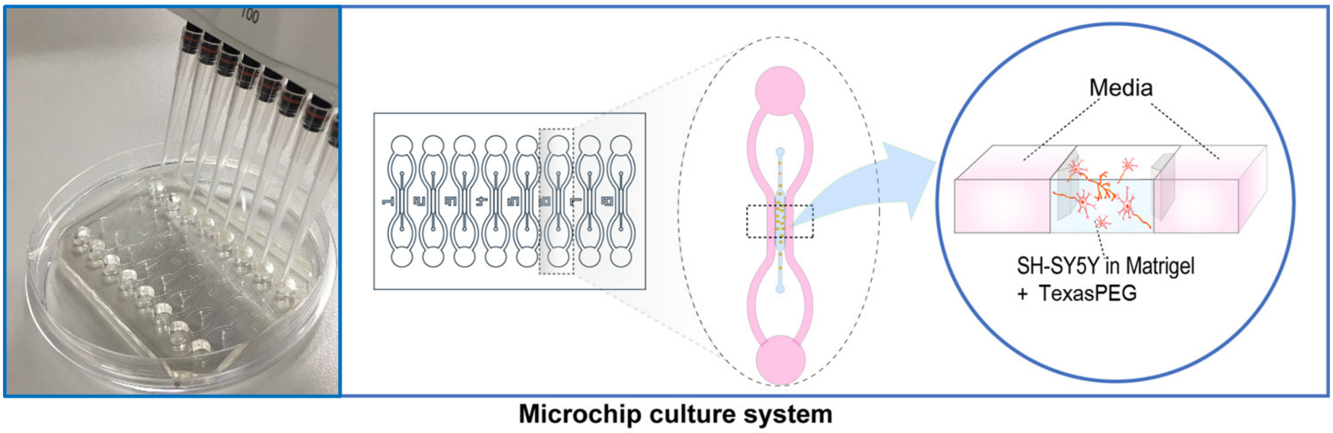

Figure 2 The microfluidic device and experimental scheme of 3D culture.
The channel dimension for gel is 1.2 mm wide, 16 mm long and the media channel is 1 mm wide, 33 mm long, respectively. A single pair of reservoirs (6 mm in diameter) is shared at the end of the two media channels.

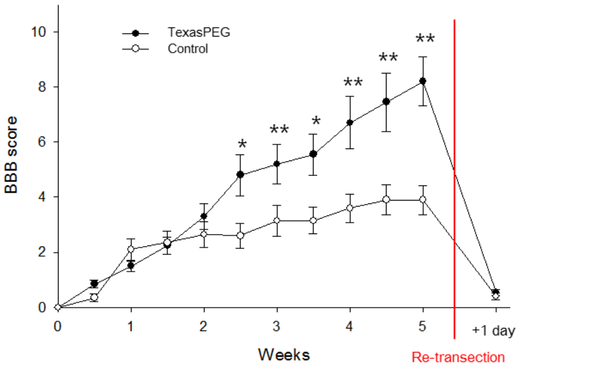

Figure 3 Locomotor function assessment in each group of animals.
Locomotor function recovery was evaluated using the Basso Beattie Bresnahan (BBB) locomotor rating scale for 5 weeks + 1 day. The re-transection time is indicated by a red line. *P < 0.05, **P < 0.01, *vs.* control group (n =10 for each group). Data are expressed as the mean ± SEM.

motor neurons and triggering a motor response (Canavero, 2015; Canavero et al., 2016). Actually, animal and human data prove that ~5–20% of these fibers are enough for motor function to unfold (Canavero, 2015; Canavero et al., 2016). This is made possible by the existence of a parallel cellular, gray matter-based network of interneurons extending from the brainstem to the spinal cord and inputted by fibers from cortical motor areas that simultaneously conveys commands to motoneurons (Canavero, 2015; Canavero et al., 2016). This short-fiber Cortico-TruncoReticulo-ProprioSpinal pathway (CTRPS) embeds and links the Central Pattern Generators located in the cervical and lumbar cord (Canavero, 2015; Canavero et al., 2016).

Such anatomical configuration explains the action of fusogens. The minimally disruptive severance of the spinal cord damages a very thin layer of these interneurons; the fusogen/sealant reseals their membranes and curbs cell death (Ye et al., 2016). These same cells, along with others in proximity which were not damaged by the extra-sharp blade, can immediately regrow (sprout) their appendages and reestablish contact between the apposed interfaces. Consequently, the gray matter neuropil is restored by spontaneous regrowth of the severed axons/dendrites over very short distances at the point of contact between the apposed cords.

Fusogens are applied immediately after severing the spinal cord; no astrocytic scar is thus in place to hinder the process, since a scar only becomes visible after about 1 week of injury. The astrocytic scar has been shown to promote axon regrowth in the early stage of SCI; it is only past the subacute stage that the scar slowly becomes nonpermissive (Raposo and Schwartz, 2014; Anderson et al., 2016). However, by the time the scar becomes nonpermissive, fibers will have already had time to cross the fusion interface and "bridge" the two stumps. In this study, we evaluated the effects of TexasPEG on astrocyte-driven scarring by GFAP analysis. In the control group, a strong astrocytic reaction was visible both at the site of injury and in the border area. In addition, the activity of astrocytes in the TexasPEG group was remarkably attenuated at the border area. In the latter group, GFAP immunoreactivity was weak, highly homogeneous and the astrocytic branches extended evenly throughout. In other words, the scar was apparently dialled down. On NF200 (measured in white matter) staining, the axons of neurons in the TexasPEG group branched out extensively; this confirms *in vivo* the previously reported graphene-fostered growth of neurons in *in vitro* experiments (Sahni et al., 2013). To confirm this accurately, we evaluated the acceleration of neuronal cell growth by graphene using 3D rather than conventional 2D cell cultures in which only one side is exposed; 3D cultures better simulate the *in vivo* environment. Consequently, we demonstrated the efficacy of graphene on neurite growth of SH-SY5Y cells in the TexasPEG group, using our own 3D culture kit.

An important finding was that maximal BBB scores were only in the 8 range on the BBB scoring sheet at the end of 5 weeks of recovery period. This is much lower than the 18–22 BBB (or modified BBB) score range we have previously reported (different animals) applying PEG to cords severed at the C_5 and T_9 levels. This is most likely due to poor perfu-

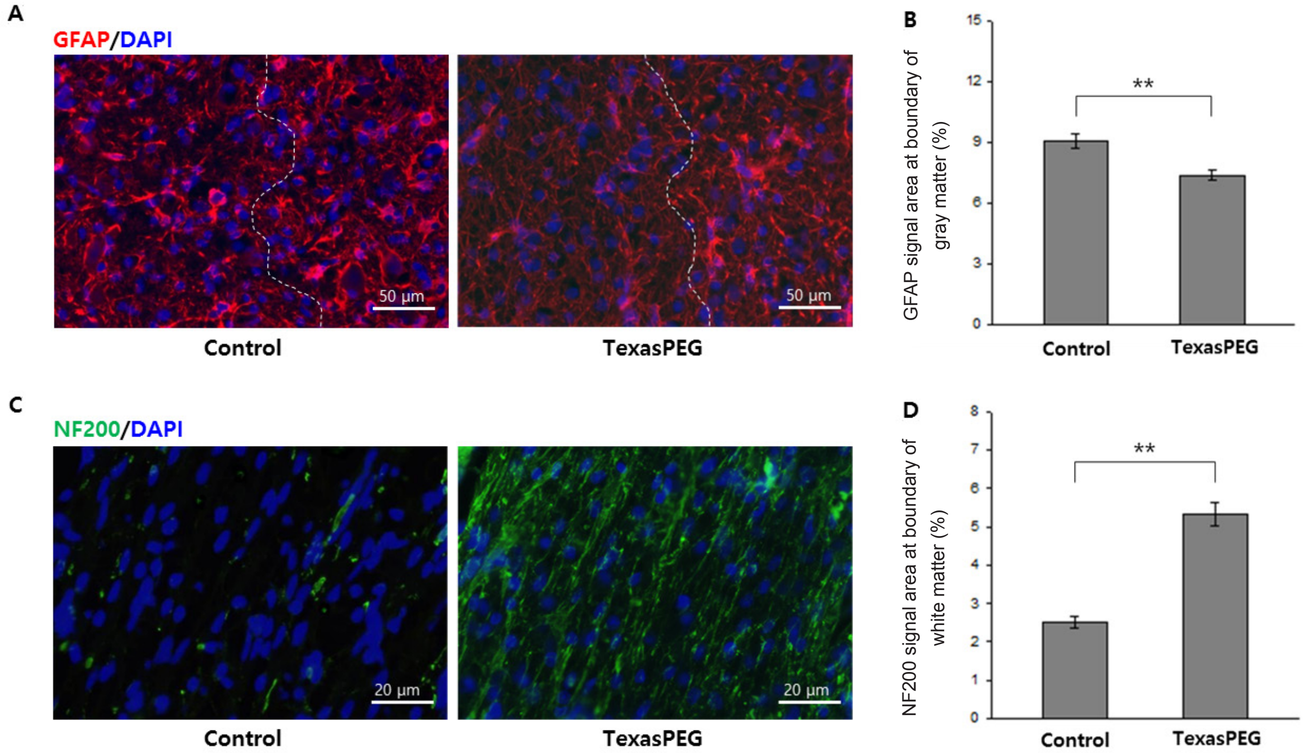

Figure 4 Glial scar formation in the gray matter and axonal regrowth in the white matter of the lesion area (immunofluorescence microscopy).
(A) Representative images of the GFAP (red) and DAPI (blue) immunofluorescence in the lesion area at 5 weeks. Dashed lines delineate the boundary area (dashed right) and the periphery (dashed left). Scale bars: 50 μm. (B) Quantitative analysis of the percentage of GFAP immunoreactive area. (C) Representative images of the NF200 (green) and DAPI (blue) immunofluorescence in the lesion area at 5 weeks. Scale bars: 20 μm. (D) Quantitative analysis of the percentage of NF200-immunoreactive area. $**P < 0.01$ (independent samples t-test, $n = 10$ for each group). Data are expressed as the mean ± SEM. GFAP: Glial fibrillary acidic protein; NF200: neurofilament 200.

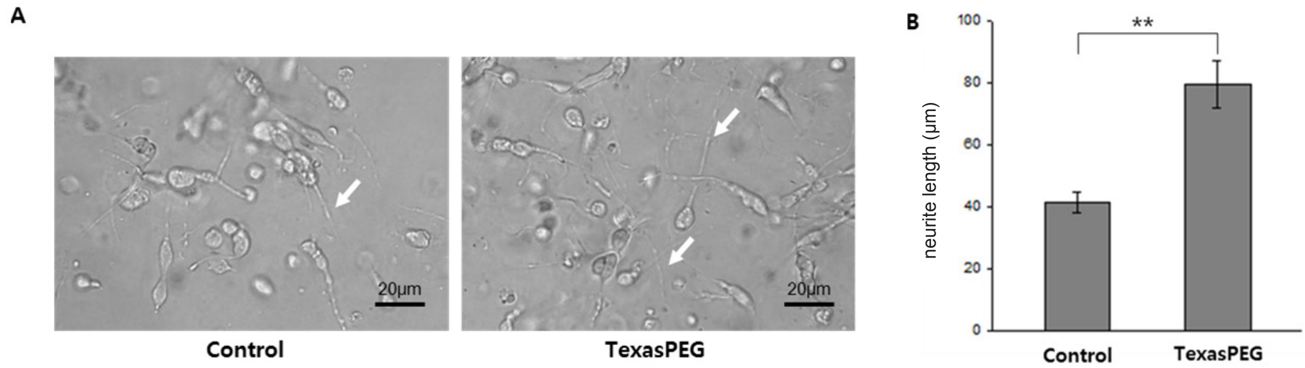

Figure 5 Neurite growth of SH-SY5Y cells *in vitro* (contrast microscopy).
(A) Differential interference contrast images were captured at 200× magnification. Arrows show neurite growth of SH-SY5Y cells. Scale bars: 20 μm. (B) Quantitative analysis of neurite growth. $**P < 0.01$ (independent samples t-test, $n = 3$ for each group). Data are expressed as the mean ± SEM.

sion below the level of the L_1 lesion. This was demonstrated by the extensive atrophy of the spinal cord below the lesion site, and such atrophy had not been observed in our prior cervical and T_9 lesion studies (unpublished observations). Spinal levels C_5 and T_9 have both caudal and rostral blood perfusion, whereas the L_1 level has rostral perfusion only. As the medullary artery (lumbosacral artery) at $T_{11–12}$ is cut with this L_1 lesioning method, blood flow to the spinal cord will cease caudally to the lesion. The atrophy of the spinal cord distal to the L_1 lesion is therefore attributed to a lack of blood flow (ischemia). This makes the observed level of recovery even more astounding: TexasPEG appears to be so pro-regnerative that even under suboptimal conditions it still can foster regrowth and recovery.

In conclusion, we have shown that the paralysis following full severance of the L_1 spinal cord can be partially reversed by immediate application of a fusogen. By severing the spinal cord without inflicting gross damage, fibers in the TPRS core can sprout rapidly before a scar forms and reconstitute the cellular "bridge" that conveys motor commands. TexasPEG treatment attenuates glial scar formation and fosters profuse axonal grow in the periphery of the spinal lesion.

While transections (*e.g.*, stab wounds) are very rare in man, the importance of this study lies in confirming the feasibility of a SCI cure modeled along the lines envisioned by Freeman.

Author contributions: *CYK, JW, RD and SC wrote the manuscript and prepared Figures 2–5. WKAS and JMT made the TexasPEG. JAK and HMC made the 3D microfluidic chip and prepared Figure 1. CYK and JK did the in vivo and in vitro experiments. AM did statistical analysis. All authors approved the final version of this paper.*

Conflicts of interest: *The authors did not report any conflicts of interest.*

Financial support: *This research was supported by a grant from the National Research Foundation (NRF) funded by the Korean government (NRF-2015M3A9C7030091 and NRF-2015R1C1A1A02037047).*

Institutional review board statement: *The experiment was approved by the Institutional Animal Care and Use Committee of the Konkuk University (No. KU15135).*

Data sharing statement: *Datasets analyzed during the current study are available from the corresponding author on reasonable request.*

Plagiarism check: *Checked twice by iThenticate.*

Peer review: *Externally peer reviewed.*

Open peer reviewer: *David Parker, University of Cambridge, UK.*

Additional files:

Additional file 1: *Open peer review report 1.*

Additional Figure 1: *Stereoscopic iamges of reconnected spinal cord of L_1 transection model at 5 weeks after surgury (test samples without re-transection).*

Additional Figure 2: *Hematoxylin-eosin staining iamges of spinal cord after re-transection (random samples, 5 weeks +1 day).*

References

Anderson MA, Burda JE, Ren Y, Ao Y, O'Shea TM, Kawaguchi R, Coppola G, Khakh BS, Deming TJ, Sofroniew MV (2016) Astrocyte scar formation aids central nervous system axon regeneration. Nature 532:195-200.

Basso DM, Beattie MS, Bresnahan JC (1995) A sensitive and reliable locomotor rating scale for open field testing in rats. J Neurotrauma 12:1-21.

Canavero S (2013) HEAVEN: The head anastomosis venture project outline for the first human head transplantation with spinal linkage (GEMINI). Surg Neurol Int 4:S335-342.

Canavero S (2015) The "Gemini" spinal cord fusion protocol: Reloaded. Surg Neurol Int 6:18.

Canavero S, Ren X (2016) Houston, GEMINI has landed: Spinal cord fusion achieved. Surg Neurol Int 7:S626-628.

Canavero S, Ren X, Kim CY, Rosati E (2016) Neurologic foundations of spinal cord fusion (GEMINI). Surgery 160:11-19.

Freeman L (1963) Observation on the Regeneration of Spinal Axons in Mammals. Proceedings, X Congreso Latinoamericano de Neurochirurgia Editorial Don Bosco:135-144.

Goldsmith HS, Fonseca A, Jr., Porter J (2005) Spinal cord separation: MRI evidence of healing after omentum-collagen reconstruction. Neurol Res 27:115-123.

Kim CY (2016) PEG-assisted reconstruction of the cervical spinal cord in rats: effects on motor conduction at 1 h. Spinal cord 54:910-912.

Kim CY, Oh H, Hwang IK, Hong KS (2016a) GEMINI: Initial behavioral results after full severance of the cervical spinal cord in mice. Surg Neurol Int 7:S629-631.

Kim CY, Oh H, Ren X, Canavero S (2017a) Immunohistochemical evidence of axonal regrowth across polyethylene glycol-fused cervical cords in mice. Neural Regen Res 12:149-150.

Kim CY, Hwang IK, Kim H, Jang SW, Kim HS, Lee WY (2016b) Accelerated recovery of sensorimotor function in a dog submitted to quasi-total transection of the cervical spinal cord and treated with PEG. Surg Neurol Int 7:S637-640.

Kim CY, Sikkema WK, Hwang IK, Oh H, Kim UJ, Lee BH, Tour JM (2016c) Spinal cord fusion with PEG-GNRs (TexasPEG): Neurophysiological recovery in 24 hours in rats. Surg Neurol Int 7:S632-636.

Kim YH, Ha KY, Kim SI (2017b) Spinal cord injury and related clinical trials. Clin Orthop Surg 9:1-9.

Laverty PH, Leskovar A, Breur GJ, Coates JR, Bergman RL, Widmer WR, Toombs JP, Shapiro S, Borgens RB (2004) A preliminary study of intravenous surfactants in paraplegic dogs: polymer therapy in canine clinical SCI. J Neurotrauma 21:1767-1777.

Lebedev MA, Nicolelis MA (2017) Brain-machine interfaces: from basic science to neuroprostheses and Neurorehabilitation. Physiol Rev 97:767-837.

Miller LE, Zimmermann AK, Herbert WG (2016) Clinical effectiveness and safety of powered exoskeleton-assisted walking in patients with spinal cord injury: systematic review with meta-analysis. Med Devices (Auckl) 9:455-466.

Minassian K, Hofstoetter US (2016) Spinal cord stimulation and augmentative control strategies for leg movement after spinal paralysis in humans. CNS Neurosci Ther 22:262-270.

Olby NJ, Muguet-Chanoit AC, Lim JH, Davidian M, Mariani CL, Freeman AC, Platt SR, Humphrey J, Kent M, Giovanella C, Longshore R, Early PJ, Munana KR (2016) A placebo-controlled, prospective, randomized clinical trial of polyethylene glycol and methylprednisolone sodium succinate in dogs with intervertebral disk herniation. J Vet Intern Med 30:206-214.

Raposo C, Schwartz M (2014) Glial scar and immune cell involvement in tissue remodeling and repair following acute CNS injuries. Glia 62:1895-1904.

Ren S, Liu ZH, Wu Q, Fu K, Wu J, Hou LT, Li M, Zhao X, Miao Q, Zhao YL, Wang SY, Xue Y, Xue Z, Guo YS, Canavero S, Ren XP (2017) Polyethylene glycol-induced motor recovery after total spinal transection in rats. CNS Neurosci Ther 23:680-685.

Sahni D, Jea A, Mata JA, Marcano DC, Sivaganesan A, Berlin JM, Tatsui CE, Sun Z, Luerssen TG, Meng S, Kent TA, Tour JM (2013) Biocompatibility of pristine graphene for neuronal interface. J Neurosurg Pediatr 11:575-583.

Sikkema WKA, Metzger AB, Wang T, Tour JM (2017) Physical and electrical characterization of TexasPEG: An electrically conductive neuronal scaffold. Surg Neurol Int 8:84.

Silva NA, Sousa N, Reis RL, Salgado AJ (2014) From basics to clinical: a comprehensive review on spinal cord injury. Prog Neurobiol 114:25-57.

Tabakow P, Raisman G, Fortuna W, Czyz M, Huber J, Li D, Szewczyk P, Okurowski S, Miedzybrodzki R, Czapiga B, Salomon B, Halon A, Li Y, Lipiec J, Kulczyk A, Jarmundowicz W (2014) Functional regeneration of supraspinal connections in a patient with transected spinal cord following transplantation of bulbar olfactory ensheathing cells with peripheral nerve bridging. Cell Transplant 23:1631-1655.

Ye Y, Kim CY, Miao Q, Ren X (2016) Fusogen-assisted rapid reconstitution of anatomophysiologic continuity of the transected spinal cord. Surgery 160:20-25.

(*Copyedited by Li CH, Song LP, Zhao M*)